

Journal of Materials Chemistry C

Accepted Manuscript



This is an *Accepted Manuscript*, which has been through the Royal Society of Chemistry peer review process and has been accepted for publication.

Accepted Manuscripts are published online shortly after acceptance, before technical editing, formatting and proof reading. Using this free service, authors can make their results available to the community, in citable form, before we publish the edited article. We will replace this *Accepted Manuscript* with the edited and formatted *Advance Article* as soon as it is available.

You can find more information about *Accepted Manuscripts* in the [Information for Authors](#).

Please note that technical editing may introduce minor changes to the text and/or graphics, which may alter content. The journal's standard [Terms & Conditions](#) and the [Ethical guidelines](#) still apply. In no event shall the Royal Society of Chemistry be held responsible for any errors or omissions in this *Accepted Manuscript* or any consequences arising from the use of any information it contains.

(Submitted to J. Mater. Chem. C)

Intense Green-light Emission from 9,10-bis (4-(1,2,2-triphenylvinyl)styryl) anthracene Emitting Electroluminescence Devices

Shunyu Jin, Yan Tian, Fei Liu^{a,}, Jun Chen, Shaozhi Deng^{b,*}, Ningsheng Xu*

Corresponding author: ^aliufei@mail.sysu.edu.cn, ^bstsdz@mail.sysu.edu.cn

State Key Laboratory of Optoelectronic Materials and Technologies,

And Guangdong Province

Key Laboratory of Display Material and Technology,

Sun Yat-sen University, Guangzhou 510275, People's Republic of China

Abstract

Although 9,10-bis (4-(1,2,2-triphenylvinyl)styryl) anthracene (TPE-An) with excellent aggregation-induced emission (AIE) property can effectively enhance the luminescence efficiency of light-emitting materials, the practical TPE-An-emitting electroluminescence (EL) devices have not been successfully fabricated until now. In our paper, the energy-band diagram of TPE-An is determined by combination of ultraviolet-visible (UV-Vis) spectroscope and cyclic voltammetry (CV) techniques. Subsequently, space-charge-limited-current (SCLC) method is firstly used to obtain the hole mobility of TPE-An and design a better EL device structure. By the calculation, the maximum hole mobility of 50 nm TPE-An film can arrive at $4.00 \times 10^{-4} \text{ cm}^2/\text{V}\cdot\text{s}$ at 0.1 MV/cm field. Finally, TPE-An-emitting EL devices have been respectively fabricated on glass and flexible PET substrate. Both of these two EL devices exhibit an intense green-light emission at 515 nm. Moreover, the maximum luminance of EL device on glass can reach 24721.8 cd/m^2 at 10.0 V, and its maximum current efficiency is as high as 14.7 cd/A at 131.6 mA/cm^2 . It is noted that the flexible EL device on PET substrate maintains a stable emission and nice working performance even if the bending angles arrives at 140° . Therefore, it suggests that TPE-An should have a promising future in EL device applications.

Key words: TPE-An, SCLC technique, hole mobility, electroluminescence (EL), flexible device

1. Introduction

Since electroluminescence (EL) device of organic materials were firstly fabricated in the 1960s [1], much effort has been devoted to improving the work efficiency of EL devices by different methods, such as optimizing the device structures or finding excellent light-emitting materials [2-6]. But for most luminescent materials with conventional π -conjugated planar chromophores, the aggregation-caused quenching (ACQ) effect usually emerges when they form thin film. In this situation, the light emissions from the film of common luminescent material are weakened to great extent, which has hold back their applications in EL devices. This problem has not been solved until a new aggregation-induced emission (AIE) material, i.e., silole molecule, emerged in 2001 [7]. Because AIE materials successfully overcame the shortage of the aggregation-caused quenching (ACQ) effect, they got a rapid development in the last decade [8-11]. The luminescence efficiency of EL device will be significantly improved if AIE material is used as emitting layer [12-15]. Among the reported AIE fluorophores, tetraphenylethene (TPE) is very unique because it possesses obvious AIE behaviors, which reveals TPE-based AIE materials have potential applications in EL device [15, 16]. As a famous member of TPE derivatives, 9,10-bis(4-(1,2,2-triphenylvinyl)styryl) anthracene (TPE-An) exhibits very fascinating AIE characteristics, which has attracted considerable attention [14].

It is known to us all that the emitting layer with high carrier mobility is indeed needed for high EL performance. So determining the carrier mobility of TPE-An film at varied field is the prerequisite for designing excellent TPE-An-emitting EL device. To our knowledge, many techniques have been used to measure the carrier mobility of organic film, such as time of flight (TOF), field effect transistor (FET) and transient EL methods [17, 18]. TOF and FET methods are only suitable for measuring thick film (2 μm ~8 μm) rather than thin film (10 nm~1 μm). The common thickness of organic emitting layer is usually smaller than 100 nm in EL device. Therefore, TOF or FET methods are not applied to measure the carrier mobility of thin film. And transient EL technique is commonly used to measure the mobility of minor carriers, which is also not suitable for determining the major carriers in organic emitting materials. Compared with other methods, space-charge-limited current (SCLC) technique is a more effective method to determine the mobility of major carrier in organic emitting layers with sub-micrometer thickness [19-21]. Most importantly, SCLC measurement can be used to calculate the carrier mobility at varied electric field, which is more helpful for simulating the practical performance of thin film under working conditions. However, SCLC method has not been applied to investigate the hole mobility of TPE-An until now. As a result,

TPE-An-emitting EL device has not been successfully fabricated to our knowledge though they have excellent AIE properties, which has hold back the development of TPE-An in EL area. Therefore, it has provided challenges for researchers to apply SCLC technique to determine the major carrier mobility of TPE-An and fabricate TPE-An-emitting EL device with high performance.

In this paper, the SCLC technique is firstly used to investigate the hole mobility of TPE-An film at varied fields. Based on the energy-band diagram of TPE-An and the SCLC results, we have successfully fabricated TPE-An-emitting EL device on glass and polyethylene terephthalate (PET) substrates. Finally, the working performances of these two EL devices were respectively investigated to value their application feasibilities in display areas.

2. Experimental section

As shown in Fig. S1, the known Wittig-Horner reaction route was adopted to synthesize pure TPE-An powders, which is the same with the synthesis route in Ref. [14]. To confirm their chemical compositions, the mid-infrared spectrum, ^1H nuclear magnetic resonance (NMR) spectrum and photoluminescence (PL) spectrum of TPE-An powders are respectively provided in Figs. S2-S4. CV measurement was carried out in dichloromethane (DCM) solution (AR, >99%). The SCLC-testing devices were fabricated on indium tin oxide (ITO) glass with a sheet resistance of $14 \Omega/\text{sq}$, and the detailed fabrication procedure of SCLC device can be seen as follows. Firstly, oxygen plasma was employed to remove excess moisture on the surface of ITO glass. Subsequently, TPE-An film was deposited on ITO glass substrate by a simple thermal vapor deposition way. The base pressure of the chamber was kept at 5×10^{-4} Pa during the growth process. The morphology and work function of TPE-An (15 nm) film on ITO glass substrate was provided in Figs. S5 and S6, respectively. The multilayered SCLC-testing device was consisted of ITO/ C_{60} (2.5 nm)/TPE-An (d nm)/Al (100nm), in which the thickness (d) of TPE-An film was respectively 25, 40, 50, 60, 80, 100, 150, 200, 300 and 400 nm. The growth rate of C_{60} (Niche Fine Tech., 99%), TPE-An and Al film was adopted to be $1 \text{ \AA}/\text{sec}$, $1 \text{ \AA}/\text{sec}$ and $5 \text{ \AA}/\text{sec}$, respectively. The current-voltage (I-V) characteristics of the devices were recorded by a programmable picoammeter (Keithley 236).

The fabrication process of TPE-An-emitting EL devices on glass and PET substrate are depicted as follows. ITO substrate was respectively cleaned by acetone, ethanol and deionized water in ultrasonic cleaner before it was handed into the chamber. Subsequently, ITO substrate was treated by ten minutes` oxygen plasma to

get a clean and dry surface. The multilayered EL device was fabricated on glass substrate with the configuration of ITO/NPB (40 nm)/TPE-An (15 nm)/TPBi (10 nm)/Alq₃ (20 nm)/LiF (1 nm)/Al (100 nm). In this device structure, N,N-bis(1-naphthyl)-N,N'-diphenyl-1,1,1'-biphenyl-4,4'-diamine (NPB, Aglaia Tech., 99.9%), TPE-An, 1,3,5-tris(nphenylbenzimidazol-2-yl)benzene (TPBi, Aglaia Tech., 99.5%) and tris(8-hydroxyquinolino) (Alq₃, Aglaia Tech., 99.9%) served as hole-transporting layer (HTL), emitting layer (EL), hole-blocking layer (HBL) and electron transporting layer (ETL), respectively. And LiF/Al layer was used as the cathode, in which LiF was used as the electron injection layer of EL device. All the deposition rates of organic materials were 1 Å/sec. The deposition rate of LiF (Aladdin Industrial Inc., 99.99%) and Al was respectively kept at 0.2 Å/sec and 5 Å/sec. After deposition, the active area of the EL device was calculated to be 0.3 cm² (0.5 cm×0.6 cm). The device structure of flexible EL device on PET substrate is very similar with that of the EL device on glass substrate, and the only difference was that PET was chosen as the substrate instead of ITO glass. The current-voltage-luminescence (I-V-L) characteristics and EL spectra of TPE-An-emitting devices were studied in ambient condition by a programmable picoammeter (Keithley 236) and photometer (ST-86LA). Photoluminescence (PL) test was performed on HORIBA JY Fluorolog-3 spectrometer ($\lambda=365$ nm), and the fluorescence quantum yield of TPE-An in the solid state was determined by using a calibrated integrating sphere system.

3. Results and discussion

High carrier mobility is a very important criterion for choosing an excellent emitting layer of EL device. Before the SCLC technique was performed on the TPE-An devices, it is necessary to explore the energy-band diagram in advance for designing a favorable configuration of SCLC-testing device. Here, UV-Vis absorption spectroscopy and CV method were combined together to ascertain the band diagram of TPE-An. Figure 1(a) shows the UV-Vis spectrum of TPE-An. The onset of the absorption peak was found to locate at 479 nm. Based on the Einstein equation of $\lambda = hc/E$, bandgap (E_g) can be obtained to be 2.59 eV. Based on our previous research, the HOMO-LUMO gap of TPE-An in the powders and in the film are comparable [24]. The CV curve of TPE-An is given in Figure 1(b). From Fig. 1(b), TPE-An can be confirmed to be electrochemically active. Referred by the reference potential of ferrocene [22, 23], the HOMO of TPE-An can be worked out to be 5.25 eV. Based on the relationship among the HOMO, LUMO and E_g , the LUMO level of TPE-An can be deduced to be 2.66 eV because E_g has been worked out to be 2.59 eV by UV-Vis technique. Combined the obtained HOMO with LUMO results, the band diagram of

TPE-An is given in Fig. 1(c).

Formation of an ohmic or quasi-ohmic contact between TPE-An film and ITO substrate was very necessary for accurately determining the carrier mobility in the following SCLC experiments. Herein, 2.5 nm buckminsterfullerene (C_{60}) film was chosen as the buffer layer to form a quasi-ohmic contact between TPE-An and substrate by because the use of C_{60} can effectively decrease the work function difference between ITO and TPE-An film [25, 26]. Moreover, the use of C_{60} will do good for enhancing the hole injection because C_{60} has a similar carrier mobility with TPE-An. As seen in Fig. S7, the I-V curves of the ITO/ C_{60} (2.5 nm)/TPE- An (100 nm) are nearly linear, which proves the quasi-ohmic contact has been established between the ITO and TPE-An layer as we expected. Al was chosen as the cathode of TPE-An SCLC-testing devices because its Fermi level is far lower than that of the LUMO of TPE-An. In this situation, the existence of large barrier between the Fermi level of Al and the LUMO of TPE-An prevents the electrons from injecting into TPE-An film based on the classical energy-band theory. Therefore, ITO/ C_{60} (2.5 nm)/TPE-An (d nm)/Al (100nm) configuration was finally chosen as the hole-injection device for SCLC measurements. In our experiments, TPE-An film was grown in different thickness to study the effect of thickness on the carrier mobility. The working mechanism of the SCLC technique is based on the classical SCLC equation, which can be described as [27]:

$$J = \frac{9}{8} \varepsilon_0 \varepsilon \mu \frac{E^2}{d} \quad (1)$$

, where E is the applied electric field, d is the thickness of the organic layer, μ is the carrier mobility, ε_0 is the permittivity of free space and ε is the relative dielectric constant. According to Eq. (1), the relationship between $\ln J$ and $\ln E$ can be deduced as:

$$\ln J = \ln \frac{9\varepsilon_0\varepsilon\mu}{8d} + 2 \ln E \quad (2)$$

From Eq. (2), $\ln J$ is proportional to $\ln E$ and the slope of $\ln J$ - $\ln E$ curve is 2, which is the key proof for SCLC behaviors of organic film.

Figure 2(a) shows the current density-voltage (J-V) characteristics of TPE-An film with various thickness. It is obviously seen that the J-V curves of all SCLC devices can be divided into two different regions. At low voltage, it exhibits a clear Schottky-diode behavior, in which J has an exponential relationship with voltage. But with the increase of applied voltage, a sudden change occurred on the J-V curves of TPE-An, as found in Fig. 2(a). As shown in Fig. 2 (b), all the $\ln J$ - $\ln E$ curves at high voltage (≥ 1 V) are proven to be almost

linear by calculating the J-V data in Fig. 2(a). In addition, the average slope of $\ln J - \ln E$ curves can be calculated to be 2.14 ± 0.09 , which meets the key proof of SCLC behaviors in Eq. (2). So it suggests that relationship between current density and applied field should conform to the SCLC model in our experiments.

It is known that the carrier mobility is dependent on the applied electric field. Some reports have referred that carrier mobility is also affected by the energy disorder due to the interaction of each hopping charge with randomly-oriented or randomly-located dipoles in the organic film [28, 29]. As a result, the effect of the energy disorder on hole mobility has to be considered to obtain more accurate mobility in our experiments. Here, we need to resort to the Poole-Frenkel (PF) equation:

$$\mu(E) = \mu_0 \exp(\beta\sqrt{E}) \quad (3)$$

, where μ_0 is the zero-field mobility, E represents the applied field, and β is Poole-Frenkel factor. The magnitude of β reflects the degree of disorder, and a smaller β suggests a lower energy disorder, which corresponds to a more ordered distribution of the energy level. Combined Eq. (1) with Eq. (3), the field-dependent SCLC equation can be easily derived as:

$$J_{SCLC} = \frac{9}{8} \varepsilon_0 \varepsilon \frac{E^2}{d} \mu_0 \exp(\beta\sqrt{E}) \quad (4)$$

Then, the expression of $\ln(J/E^2)$ can be easily obtained, which can be described as:

$$\ln\left(\frac{J}{E^2}\right) = \beta\sqrt{E} + \ln\left(\frac{9\varepsilon\varepsilon_0\mu_0}{8d}\right) \quad (5)$$

Based on Eq. (5), $\ln(J/E^2)$ is observed to have a linear relationship with \sqrt{E} , and the corresponding curve is shown in Fig. 2(c). Because the permittivity ε_0 of vacuum is 8.85×10^{-12} F/m, the Poole-Frenkel factor β and zero-field mobility μ_0 can be respectively determined by calculating the slope and the intercept of $\ln(J/E^2) - \sqrt{E}$ curve, as summarized in Table I.

To comprehend the effect of TPE-An's thickness d on μ_0 , the μ_0-d curve is given in Fig. 2(d). And the device configuration for SCLC measurements was shown in the inset. It is found that μ_0 has a nonlinear relationship with d and there exist two critical d values in the whole μ_0-d curve. When d is smaller than 50 nm, μ_0 increases from 7.92×10^{-5} to 3.99×10^{-4} cm²/V·s. But when d is bigger than 50 nm, μ_0 will continuously decrease with the increase of the thickness d of TPE-An film until d arrives at 200 nm. If d is over 200 nm,

μ_0 reaches a saturation value of $4.33 \times 10^{-6} \text{ cm}^2/\text{V}\cdot\text{s}$ and becomes insensitive to d .

Determining the carrier mobility of TPE-An at varied field is very essential for their practical applications in EL devices. Based on Eq. (3), we can calculate the hole mobility at different electric fields. Figure 3(a) gives the curve of hole mobility versus the thickness of TPE-An at 0.1 MV/cm field (a commonly-used working field of EL device). And typical atomic force microscopy (AFM) images of TPE-An film with 50 nm is provided in the inset. The hole mobility μ at various field can be deduced based on Eq. (3) because μ_0 and β has been obtained by Eq. (5). In Fig. 3(a), the hole mobility μ was seen to have a clear up-down-flat tendency, which is the same with the μ_0 - d curve (Fig. 2(d)). The hole mobility μ of TPE-An with different thickness at 0.1 MV/cm field is also provided in Table I. It is found that TPE-An film has the maximum hole mobility of $4.00 \times 10^{-4} \text{ cm}^2/\text{V}\cdot\text{s}$ when its thickness d is 50 nm. To better comprehend the relationship between carrier mobility and applied field, the curve of mobility versus electric field is shown in Fig. 3(b). When the thickness of TPE-An film ranges from 25 nm to 60 nm, the mobility is found to be insensitive to electric field whereas μ_0 is dependent on the thickness. But when d increases from 60 nm to 400 nm, the mobility becomes field-dependent once again. It is obviously seen that the hole mobility of TPE-An ($3.14 \times 10^{-4} \text{ cm}^2/\text{V}\cdot\text{s}$) can be comparable to that of another TPE derivative p -BTPATPE ($5.2 \times 10^{-4} \text{ cm}^2/\text{V}\cdot\text{s}$) at the same thickness of 60 nm [30]. In recent years, p -BTPATPE-emitting EL device has exhibited nice working behaviors due to its high mobility, such as a low turn-on voltage (at $1 \text{ cd}/\text{m}^2$) of 3.2 V, high luminance of $33700 \text{ cd}/\text{m}^2$ and power efficiency of 11.0 lm/W [31]. Also, the mobility of hole-transporting layer NPB (1.63×10^{-5} - $7.64 \times 10^{-4} \text{ cm}^2/\text{V}\cdot\text{s}$) is close to that of TPE-An film ($4.00 \times 10^{-4} \text{ cm}^2/\text{V}\cdot\text{s}$) [32, 33], which is helpful to transport the hole from anode to TPE-An layer. Therefore, one can expect that TPE-An-emitting EL device should have an excellent working performance.

EL devices of TPE-An were respectively fabricated on glass and PET substrate. Depending on the energy level and mobility of every film in EL device, TPE-An, NPB, TPBi, Alq₃ are served as HTL, HBL and ETL, respectively. The EL device on glass substrate adopted the configuration of ITO/NPB(40 nm)/TPE-An(15 nm)/TPBi (10 nm)/Alq₃(20 nm)/LiF(1 nm)/Al(100 nm). Figure 4(a) schematically gives the energy-band diagram of TPE-An-emitting EL device on glass substrate. The current-voltage-luminescence (I-V-L) curve of EL device on glass substrate is shown in Fig. 4(b), and the inset gives the luminescence image at 8.0 V. One can see that EL device on glass substrate exhibited a very uniform luminescence image in the whole surface of 0.3 cm^2 (referred by the red dash line in the inset). It is seen in Figure 4(b) that the turn-on voltage (at $1 \text{ cd}/\text{m}^2$) of EL device on glass substrate was 3.0 V. Moreover, the maximum luminance of EL device on

glass substrate was as high as 24721.8 cd/m^2 at 10.0 V. The current efficiency-power efficiency-current density curve of TPE-An-emitting EL device on glass is demonstrated in Figure 4(c) to reveal the ability of converting electric energy into light. And the corresponding device configuration is provided in the inset. The maximum current efficiency was found to be 14.7 cd/A at 131.6 mA/cm^2 . Also, the maximum power efficiency of the EL device arrived at 6.9 lm/W at 3.7 mA/cm^2 . In our future works, the effect of isomers on TPE-An's EL performance will be further studied because Z/E isomers of TPE derivatives may affect the emission behaviors of EL devices [16].

To ensure TPE-An is the emitting layer of EL device on glass substrate, the PL spectrum of TPE-An film and EL spectra of TPE-An-emitting device on glass substrate are compared in Fig. 5. Typical PL spectrum of TPE-An film is shown in Fig. 5(a). It is seen that TPE-An film has a clear green-light emission peak with a quantum yield of 75%, which appears at 515 nm. From the EL spectrum of device on glass substrate (Fig. 5(b)), the emission peak (515 nm) of EL device on glass substrate (515 nm), which coincides with that of TPE-An film well. It proves that the emitting layer of EL device on glass substrate should be TPE-An film. Table II lists the working performance of some other TPE derivative-emitting EL devices on glass substrate [31, 34-37]. As found in Table II, TPE-An-emitting EL device on glass substrate has a comparable working performance with other AIE EL devices with excellent emission behaviors.

Subsequently, we further explore the application feasibility of TPE-An's on flexible EL device because TPE-An film has nice mechanical properties. In contrast with other flexible substrates, PET has a low thermal expansion coefficient, high transmittance and low water absorption [38], and thus it was chosen as the flexible substrate of TPE-An-emitting EL device. The flexible EL device is composed of ITO/NPB (40 nm)/TPE-An (15 nm)/TPBi (10 nm)/Alq₃ (20 nm)/ LiF (1 nm)/Al (100 nm). All thin films in the flexible EL device were deposited on PET substrate by a simple thermal evaporation way, which is close to the fabrication process of EL device on glass substrate. The EL spectra of the flexible device before and under deformation (the bending angle is 100°) are shown in Fig. 5(b). It is clearly seen that the emission peak of 513 nm keeps unvaried before and under deformation. Figure 6(a) demonstrates that the I-V-L curve of the flexible EL device. The inset gives the typical luminescence photograph of the flexible EL device under deformation, which works at 14.0 V. As shown in Fig. 6(b), the maximum luminance and current efficiency of the flexible EL device is 338.0 cd/m^2 (at 16.0 V) and 0.4 cd/A (at 68.3 mA/cm^2), respectively. Moreover, it is worth noting that the flexible device exhibits a uniformed and excellent EL behavior at the bending angle of 33°.

The working stability of the flexible EL device under deformation is another essential task, which cares about its application developments. Typical photographs of the flexible EL device at various bending angles are provided in Fig. 7(a), which consists of a working cycle. It is found that the flexible EL device can recover the original shape after a working cycle is over. Although the maximum bending angle of the flexible EL device reaches about 140° , no damages is found in the whole measurement, which reveals that flexible TPE-An-emitting EL device has a strong enough endurance to large bending stress. The same cycles repeat 50 times to further evaluate the working stability of the flexible EL device. Luminance-bending cycle and turn-on voltage-bending cycle curves are respectively given in Fig. 7 (b). It is clearly seen that the emission luminance and turn-on voltage of the flexible EL device almost keeps unvaried after 50 cycles. Moreover, TPE-An-emitting EL device on glass or PET substrate has a promising half lifetime, as seen in Fig. S8. The half lifetime at an initial luminance of 1000 cd/m^2 is 120 h for EL device on glass and the half lifetime at an initial luminance of 200 cd/m^2 is 38 h, respectively. It suggests that flexible TPE-An-emitting EL device remains a good and stable working performance after undergoing repeatedly large deformation, which will be beneficial for its practical applications in flexible electronic devices.

Compared with the TPE-An-emitting EL device on glass substrate, the working performance of flexible device on PET substrate is relatively worse at the same voltage, and the possible reasons are explained as follows. The sheet resistance of ITO/PET ($182 \text{ } \Omega/\text{sq}$) is found to be far higher than that of ITO/glass ($14 \text{ } \Omega/\text{sq}$) in our experiments, which may cause flexible EL device has a larger contact resistance than EL device on glass substrate. Under this circumstance, the effective voltage loss at EL device on glass substrate is much higher than flexible device at the same applied voltage because less voltage drops at the interface between multilayers and substrate. Consequently, the working performance of EL device on glass substrate should be better than that of EL device on PET substrate. Although flexible TPE-An-emitting device cannot have the same excellent working performance with its corresponding EL device on glass substrate, it still exhibits a good enough performance in flexible EL devices. Therefore, TPE-An film should have a more promising future in flexible EL devices if the interface resistance can be effectively decreased.

4. Conclusion

The CV, UV-vis and SCLC techniques are combined together to design the configuration of TPE-An-emitting EL device. It is found that the hole mobility of TPE-An exhibits an up-down-flat tendency with the increasing film thickness. The maximum hole mobility of 50 nm TPE-An thin film is calculated to arrive at $4.00 \times 10^{-4} \text{ cm}^2/\text{V}\cdot\text{s}$ at 0.1 MV/cm field. TPE-An-emitting EL devices were respectively fabricated on glass and PET substrates by a simple thermal evaporation method. The EL device on glass demonstrated a very fascinating green-light emission performance. It has a maximum luminance of 24721.8 cd/m^2 (at 10.0 V) and its current efficiency is as high as 14.7 cd/A (at 131.6 mA/cm^2), which is comparable to many other TPE derivative-emitting EL devices with excellent performances. And the flexible EL device still maintains a stable and excellent luminance after 50 continuous measurement cycles, in which the maximum bending angle arrives at 140° . It is suggested that TPE-An can be a promising candidate in green-light EL applications. In addition, this research method can provide a beneficial reference for designing other high-efficiency EL device structures.

Acknowledgements

The authors are very thankful for the support of the National Basic Research Program of China (973 Program, Grant No. 2010CB327703, the National Natural Science foundation of China, Grant No. 50802117), Program for New Century Excellent Talents in University (NCET-12-0573), National Project for the Development of Key Scientific Apparatus (2013YQ12034506), the Natural Science foundation of Guangdong Province (No. S2012010010519), China Scholarship Council Fund for Young Backbone Teacher, the Science and Technology Department of Guangdong Province, the Education Department of Guangdong Province, and the Science and Technology Department of Guangzhou City.

5. Reference

- [1] M. Pope, H. P. Kallmann and P. J. Magnante, *J. Chem. Phys.*, 1963, 38, 2042.
- [2] W. Shi, S. Q. Fan, F. Huang, W. Yang, W. R. S. Liu and Y. Cao, *J. Mater. Chem.*, 2006, 16, 2387.
- [3] X. H. Zhou, Y. Zhang, Y. Q. Xie, Y. Cao and J. Pei, *Macromolecules*, 2006, 39, 3830.
- [4] W. Y. Lai, Q. Y. He, R. Zhu, Q. Q. Chen and W. Huang, *Adv. Funct. Mater.*, 2008, 18, 265.
- [5] H. Xu, K. Yin and W. Huang, *J. Phys. Chem. C*, 2010, 114, 1674.
- [6] F. P. Lu, Q. Wang and X. Zhou, *Chin. Phys. B*, 2003, 22, 037202.
- [7] J. D. Luo, Z. L. Xie, J. W. Y. Lam, L. Cheng, H. Y. Chen, C. F. Qiu, H. S. Kwok, X. W. Zhan, Y. Q. Liu, D. B. Zhu and B. Z. Tang, *Chem. Commun. Cambridge*, 2001, 1740.
- [8] J. W. Chen, C. C. W. Law, J. W. Y. Lam, Y. P. Dong, S. M. F. Lo, I. D. Williams, D. B. Zhu and B. Z. Tang, *Chem. Mater.*, 2003, 15, 1535.
- [9] Y. Q. Dong, J. W. Y. Lam, A. J. Qin, Z. Li, J. Z. Sun, H. H. Y. Sung, I. D. Williams and B. Z. Tang, *Chem. Commun. Cambridge*, 2007, 40.
- [10] Z. Li, Y. Q. Dong, B. X. Mi, Y. H. Tang, M. Häussler, H. Tong, Y. P. Dong, J. W. Y. Lam, Y. Ren, H. H. Y. Sung, K. S. Wong, P. Gao, I. D. Williams, H. S. Kwok and B. Z. Tang, *J. Phys. Chem. B*, 2005, 109, 10061.
- [11] G. Yu, S. W. Yin, Y. Q. Liu, J. S. Chen, X. J. Xu, X. B. Sun, D. G. Ma, X. W. Zhan, Q. Peng, Z. G. Shuai, B. Z. Tang, D. B. Zhu, W. H. Fang and Y. Luo, *J. Am. Chem. Soc.*, 2005, 127, 6335.
- [12] S. J. Liu, F. He, H. Wang, H. Xu, C. Y. Wang, F. Li and Y. G. Ma, *J. Mater. Chem.*, 2008, 18, 4802.
- [13] Y. Liu, X. T. Tao, F. Z. Wang, X. N. Dang, D. C. Zou, Y. Ren and M. H. Jiang, *J. Phys. Chem. C*, 2008, 112, 3975.
- [14] B. J. Xu, Z. G. Chi, J. Y. Zhang, X. Q. Zhang, H. Y. Li, X. F. Li, S. W. Liu, Y. Zhang and J. R. Xu, *Chem.-Asian. J.*, 2011, 6, 1470.
- [15] Y. Q. Dong, J. W. Y. Lam, A. J. Qin, J. Z. Liu, Z. Li, B. Z. Tang, J. X. Sun and H. S. Kwok, *Appl. Phys. Lett.*, 2007, 91, 011111.
- [16] J. Huang, N. Sun, P. Y. Chen, R. L. Tang, Q. Q. Li, D. G. Ma and Z. Li, *Chem. Comm.*, 2014, 2, 2028.
- [17] C. H. Cheung, K. C. Kwok, S. C. Tse and S. K. So, *J. Appl. Phys.*, 2008, 103, 09370.
- [18] S. Barth, P. Müller, H. Riel, P. F. Seidler, W. Rieß, H. Vestweber and H. Bässler, *J. Appl. Phys.* 2011, 89,

3711.

- [19] P. W. M. Blom, M. J. M. De Jong and J. J. M. Vlegaar, *Appl. Phys. Lett.*, 1996, 68, 3308.
- [20] L. Bozano, S. A. Carter, J. C. Scott, G. G. Malliaras and P. J. Brock, *Appl. Phys. Lett.*, 1999, 74, 1132.
- [21] T. Yasuda, Y. Yamaguchi, D. C. Zou and T. Tsutsui, *Jpn. J. Appl. Phys. Part 1*, 2002, 41, 5625.
- [22] Y. Liu, M. S. Liu and A.K.-Y. Jen, *Acta Polym.*, 1999, 50, 105.
- [23] H. Q. Zhang, S. M. Wang, Y. Q. Li, B. Zhang, C. X. Du, X. J. Wan and Y. S. Chen, *Tetrahedron*, 2009, 65, 4455.
- [24] S. Y. Jin, F. Liu, S. Z. Deng, X. Zhou, J. Chen and N. S. Xu, accepted by *Sci. Adv. Mater.*, 2015, doi:10.1166/sam.2015.2389 2014.
- [25] I. H. Hong, M. W. Lee, Y. M. Koo, H. Jeong, T. S. Kim and O. K. Song, *Appl. Phys. Lett.*, 2005, 87, 063502.
- [26] N. Hayashi, H. Ishii, Y. Ouchi and K. Seki, *J. Appl. Phys.*, 2002, 92, 3284.
- [27] V. Coropceanu, J. Cornil, D. A. S. Filho, Y. Olivier, R. Silbey and J. Bredas, *Chem. Rev.*, 2007, 107, 926.
- [28] G. G. Malliaras, J. R. Salem, P. J. Brock and C. Scott, *Phys. Rev. B*, 1998, 58, R13411.
- [29] T. Y. Chu and O. K. Song, *Appl. Phys. Lett.*, 2007, 90, 203512.
- [30] Z. J. Zhao, Z. F. Li, J. W. Y. Lam, J-L. Maldonado, G. Ramos-Ortiz, Y. Liu, W. Z. Yuan, J. B. Xu, Q. Miao and B. Z. Tang, *Chem. Commun.*, 2011, 47, 6924.
- [31] Y. Liu, S. Chen, J. W. Y. Lam, P. Lu, R. T. K. Kwok, F. Mahtab, H. S. Kwok and B. Z. Tang, *Chem. Mater.*, 2011, 23, 2536.
- [32] T. Y. Chu and O. K. Song, *Appl. Phys. Lett.*, 2007, 90, 203512.
- [33] S. C. Tse, S. W. Tsang and S. K. So, *Proc. SPIE 6333, Organic Light Emitting Materials and Devices X*, 2006, 63331P.
- [34] S. Odabas, E. Tekin, F. Turksoy and C. Tanyeli, *J. Mater. Chem. C*, 2013, 1, 7081.
- [35] W. L. Gong, B. Wang, M. P. Aldred, C. Li, G. F. Zhang, T. Chen, L. Wang and M. Q. Zhu, *J. Mater. Chem. C*, 2014, 2, 7001.
- [36] W. Z. Yuan, P. Lu, S. Chen, J. W. Y. Lam, Z. Wang, Y. Liu, H. S. Kwok, Y. Ma and B. Z. Tang, *Adv. Mater.*, 2010, 22, 2159.
- [37] L. Chen, Y. B. Jiang, H. Nie, R. R. Hu, H. S. Kwok, F. Huang, A. J. Qin, Z. J. Zhao and B. Z. Tang, *ACS Appl. Mater. Interfaces*, 2014, 6, 17215.
- [38] G. P. Crawford, *Flexible Flat Panel Displays*, Wiley, NY, 2005.

Table and Figure Captions

Table I. Zero-mobility, Pool-Frenkel factor and simulation mobility of TPE-An thin film at various thickness (at electric field of 0.1 MV/cm).

Table II. EL performance of various tetraphenylethene-emitting EL devices.

Figure 1. (a) Ultraviolet-visible absorption spectrum of TPE-An powders. (b) Cyclic voltammetry curve of TPE-An in dichloromethane. Inset: molecular structure of TPE-An. (c) Electronic structure of TPE-An.

Figure 2. (a) Current density-voltage characteristics, (b) $\ln J$ - $\ln E$ curves and (c) space-charged-limited currents of electron injection devices at various thicknesses of TPE-An. (d) Zero-field mobility (μ_0) for the hole mobility estimated by SCLC for ITO/C₆₀/TPE-An(d) /Al devices. Inset: scheme of SCLC-testing device configuration.

Figure 3. (a) Simulation curve of hole mobility versus TPE-An's thickness at electric field of 0.1 MV/cm. Inset: 1 μm \times 1 μm AFM morphology images of ITO/C₆₀/TPE-An multilayer with 50 nm TPE-An layer. Scale bar is 200 nm. (b) Mobility-square root of simulated electric field for different TPE-An thicknesses.

Figure 4. (a) Energy level diagram of multilayer EL Device of TPE-An. (b) Current density-voltage-luminance characteristics of TPE-An-emitting EL device on glass. Inset: luminescence photograph of EL device on glass taken at 8 V. The luminescing area is referred by red dash line. Scale bar: 2 mm. (c) Changes in efficiencies with the current density based on EL device on glass. Inset: configuration of EL device on glass.

Figure 5. (a) Photoluminescence spectrum of TPE-An thin film and (b) electroluminescence spectra of TPE-An-emitting EL device on glass and on PET substrates at 5 V and 14 V, respectively.

Figure 6. (a) Current density-voltage-luminance characteristics of flexible TPE-An-emitting EL device. Inset: photograph of flexible EL device taken at 14 V. (b) Changes in efficiencies with the current density in flexible EL device. Inset: configuration of flexible EL device.

Figure 7. (a) TPE-An-emitting flexible EL device images of backward and forward deformation at different bending states. (b) Maximum luminance and turn-on voltage obtained after different bending cycles.

Parameters Thickness	Zero-field mobility μ_0 (cm ² /V·s)	Pool-Frenkel factor β	Estimated mobility μ (cm ² /V·s)
25 nm	7.92×10^{-5}	1.14×10^{-4}	7.92×10^{-5}
50 nm	4.00×10^{-4}	2.76×10^{-4}	4.00×10^{-4}
100 nm	6.27×10^{-5}	1.73×10^{-3}	6.28×10^{-5}
200 nm	4.82×10^{-5}	2.1×10^{-3}	4.83×10^{-5}
400 nm	4.33×10^{-5}	2.1×10^{-3}	4.33×10^{-5}

Table I

(S. Y. Jin et al., *submitted to J. Mater. Chem. C*)

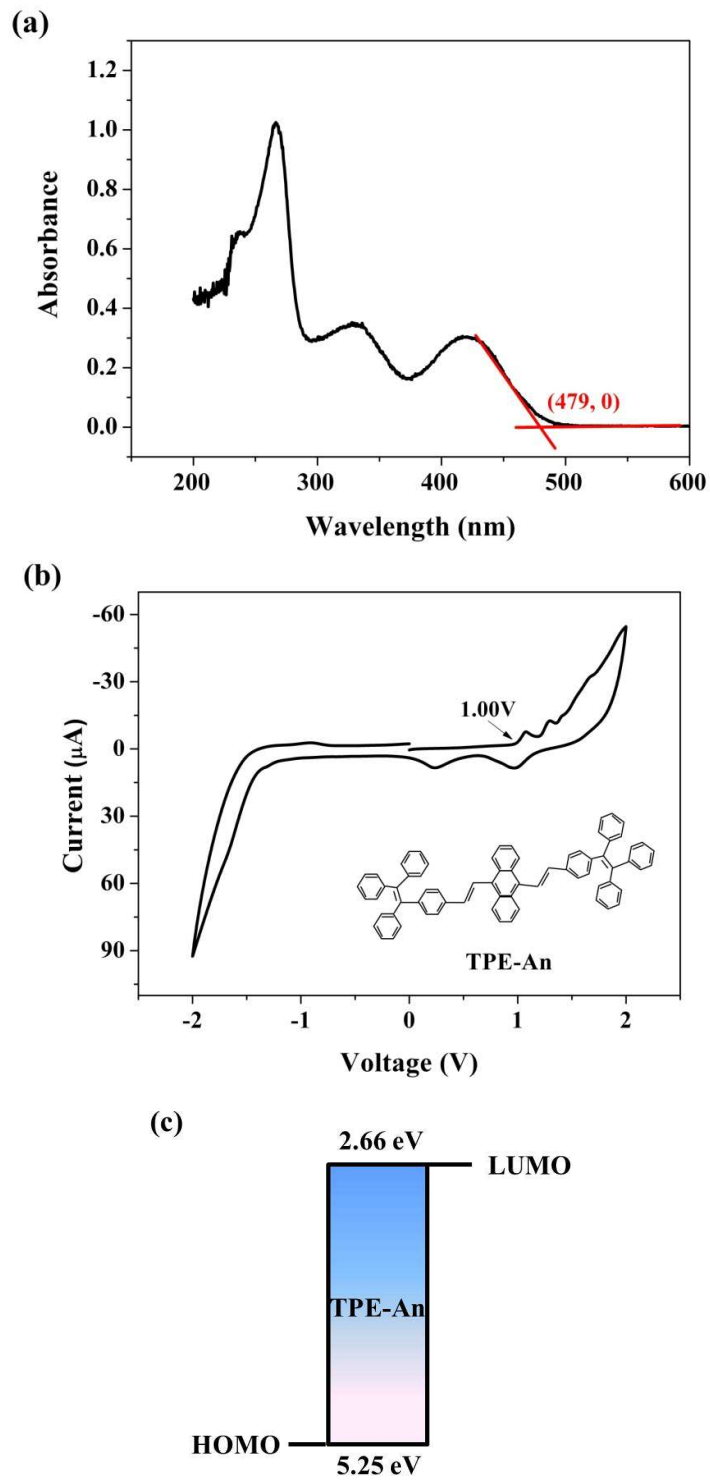
Group	Emitter	V_{on}/V	L_{max}/cdm^{-2}	η_{max}/cdA^{-1}
Y. Liu et al [31]	2TPATPE	3.2	33770 (@15 V)	13 (@4.2 V)
S. Odabas et al [34]	TIPE	5	18000 (@15 V)	5.2 (@50 mA/cm ²)
W.L.Gong et al [35]	Cz-1TPE	3.5	2585 (@9 V)	3.5 (@7 V)
W. Z. Yuan et al [36]	4TPETPA	4.1	10726 (@15 V)	8 (@5 V)
L. Chen et al [37]	TPE-PNPB	3.2	49993 (@20 V)	15.7(@3-4 V)
Our work	TPE-An	3	24721.8 (@1 V)	14.7 (@10 V)

Abbreviations: V_{on} = turn-on voltage at 1 cd /m², L_{max} = the maximum luminance,

η_{max} =the maximum current efficiency, respectively.

Table II

(S. Y. Jin et al., *submitted to J. Mater. Chem. C*)



(S. Y. Jin et al., *submitted to J. Mater. Chem. C*)

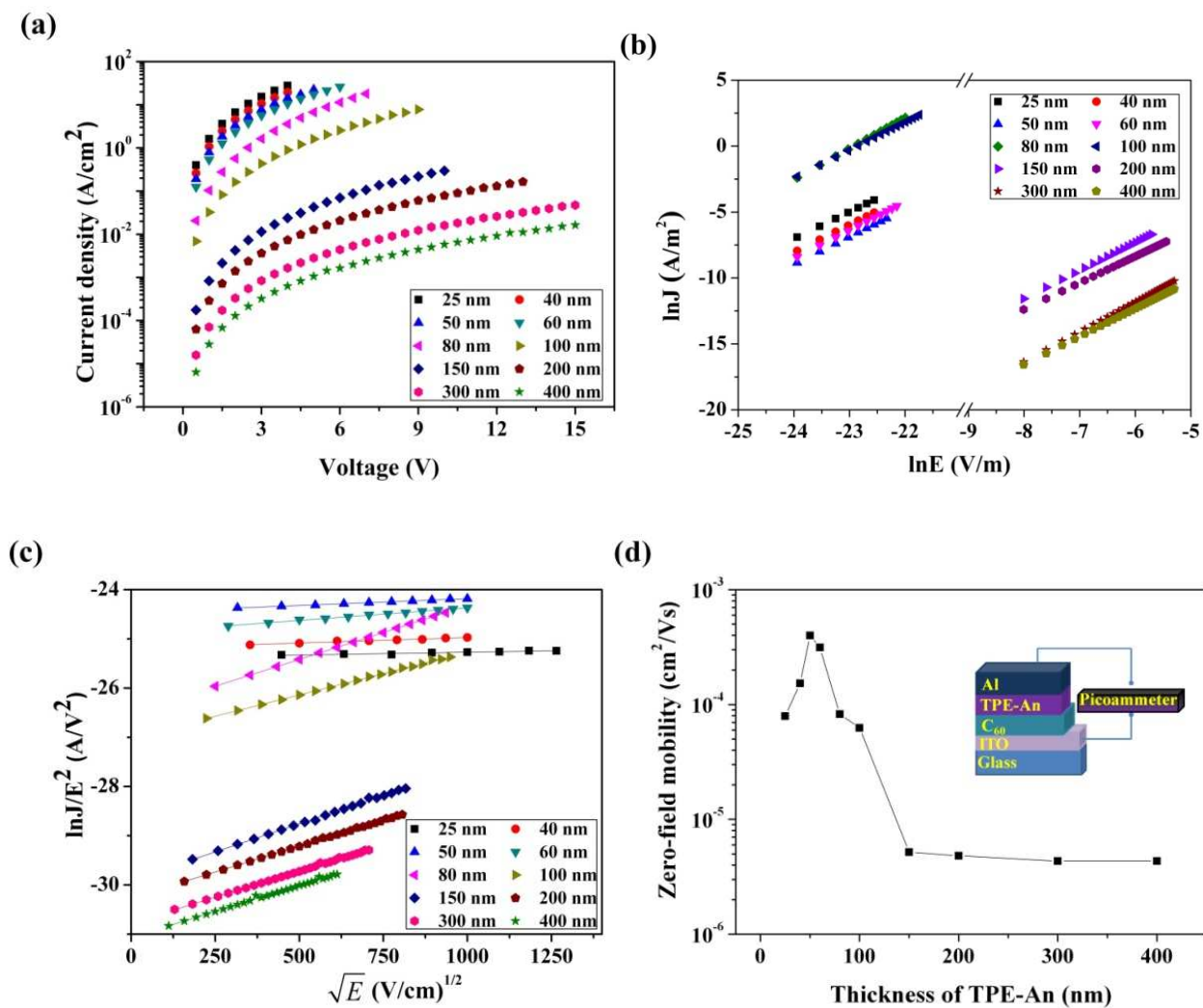


Figure 2

(S. Y. Jin et al., *submitted to J. Mater. Chem. C*)

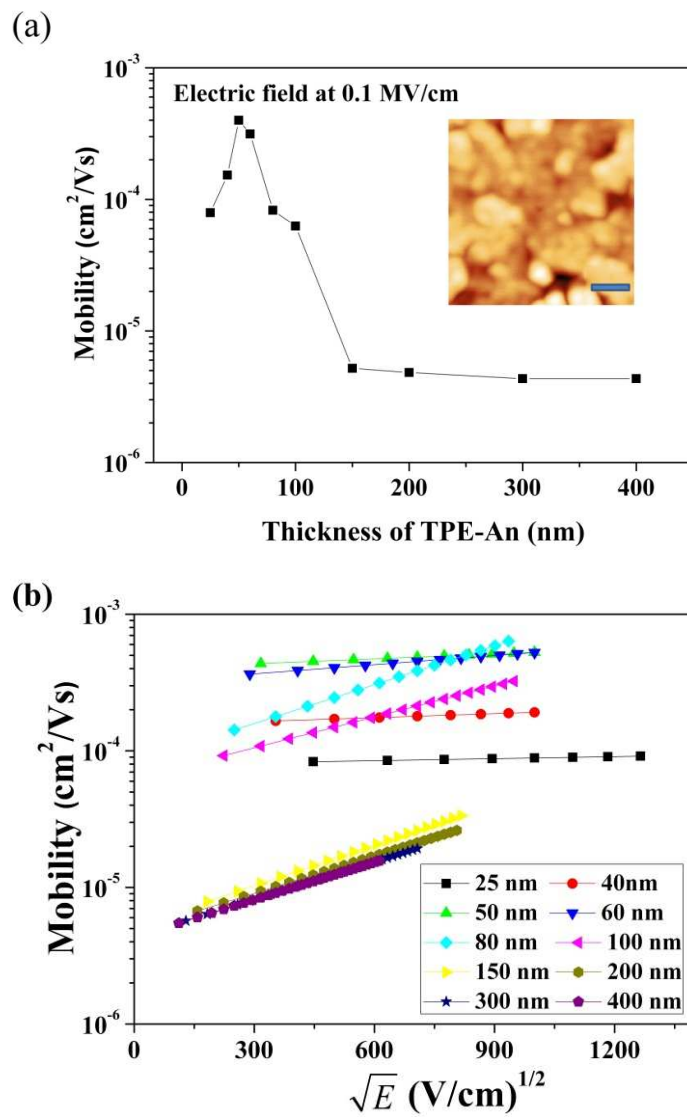


Figure 3

(S. Y. Jin et al., *submitted to J. Mater. Chem. C*)

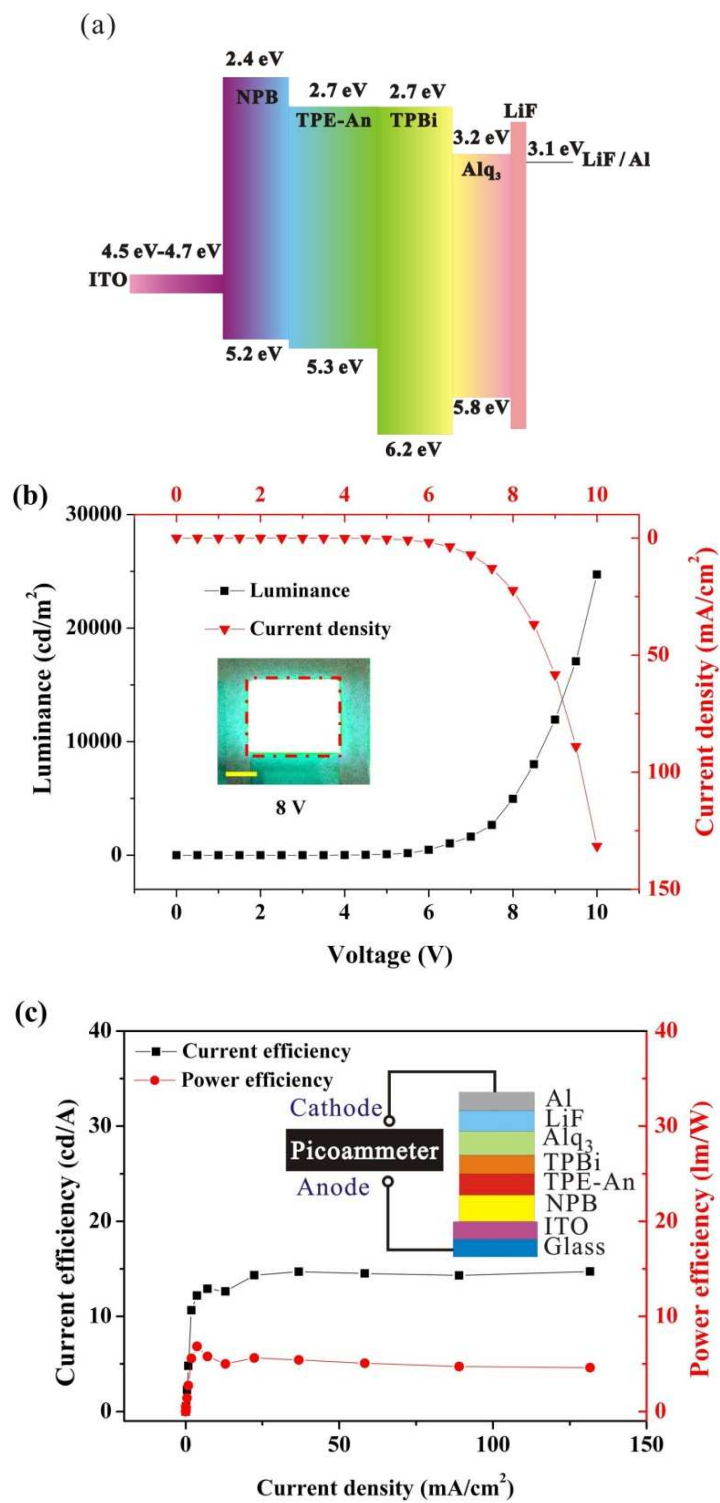


Figure 4

(S. Y. Jin et al., *submitted to J. Mater. Chem. C*)

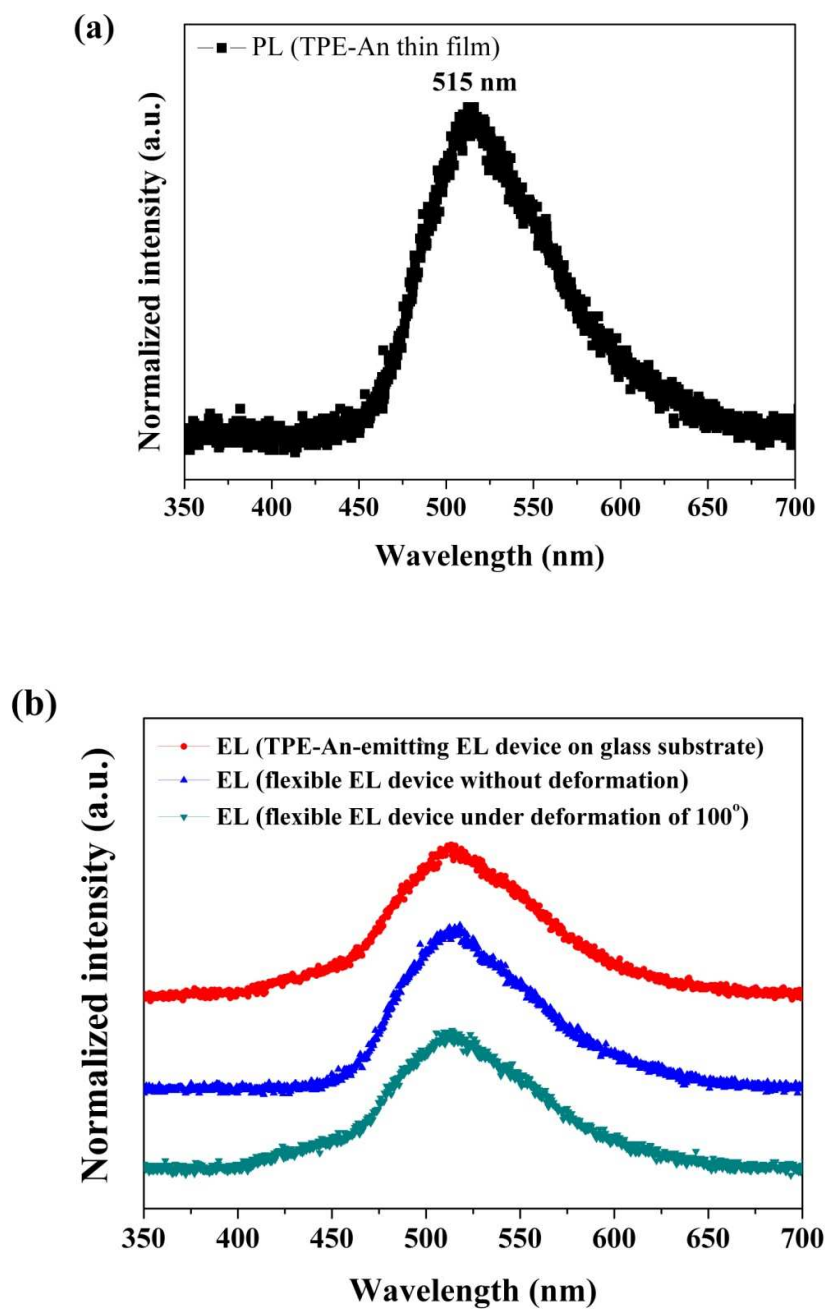


Figure 5

(S. Y. Jin et al., *submitted to J. Mater. Chem. C*)

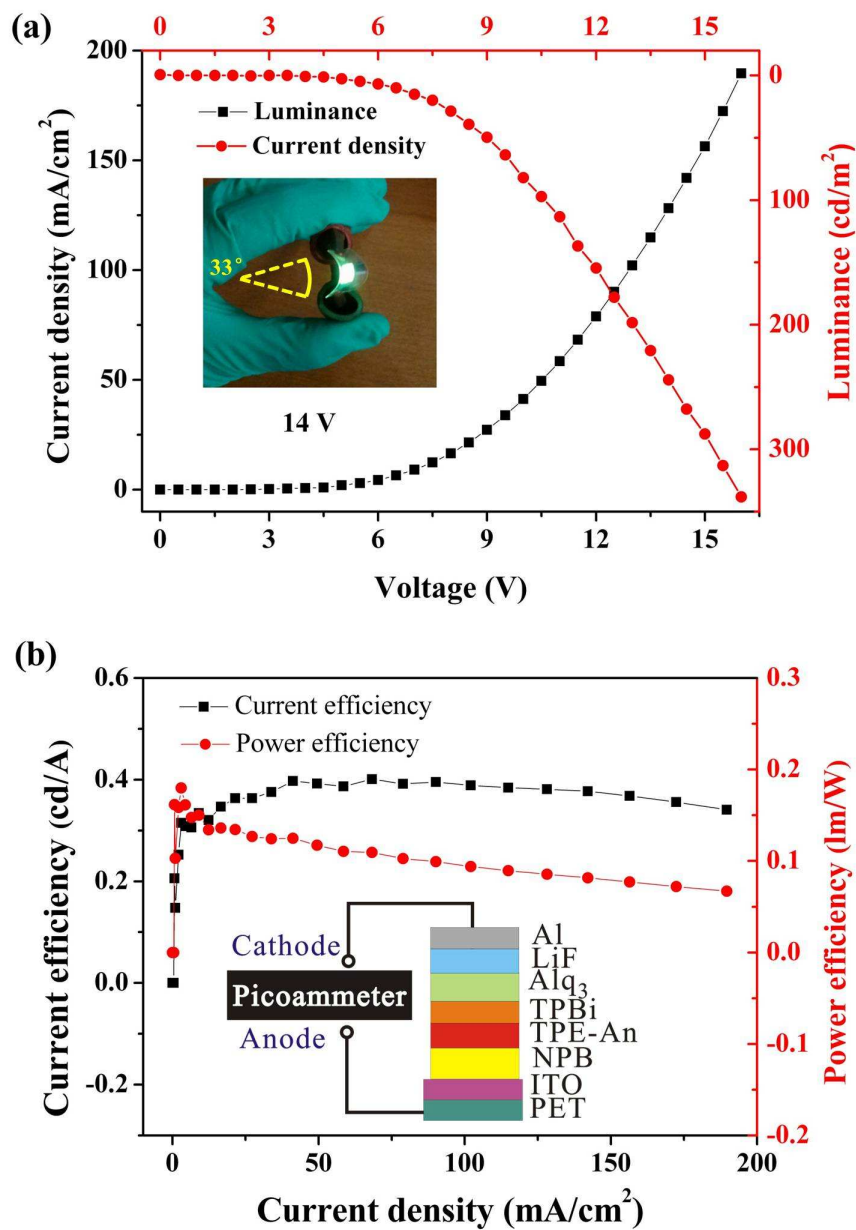


Figure 6

(S. Y. Jin et al., *submitted to J. Mater. Chem. C*)

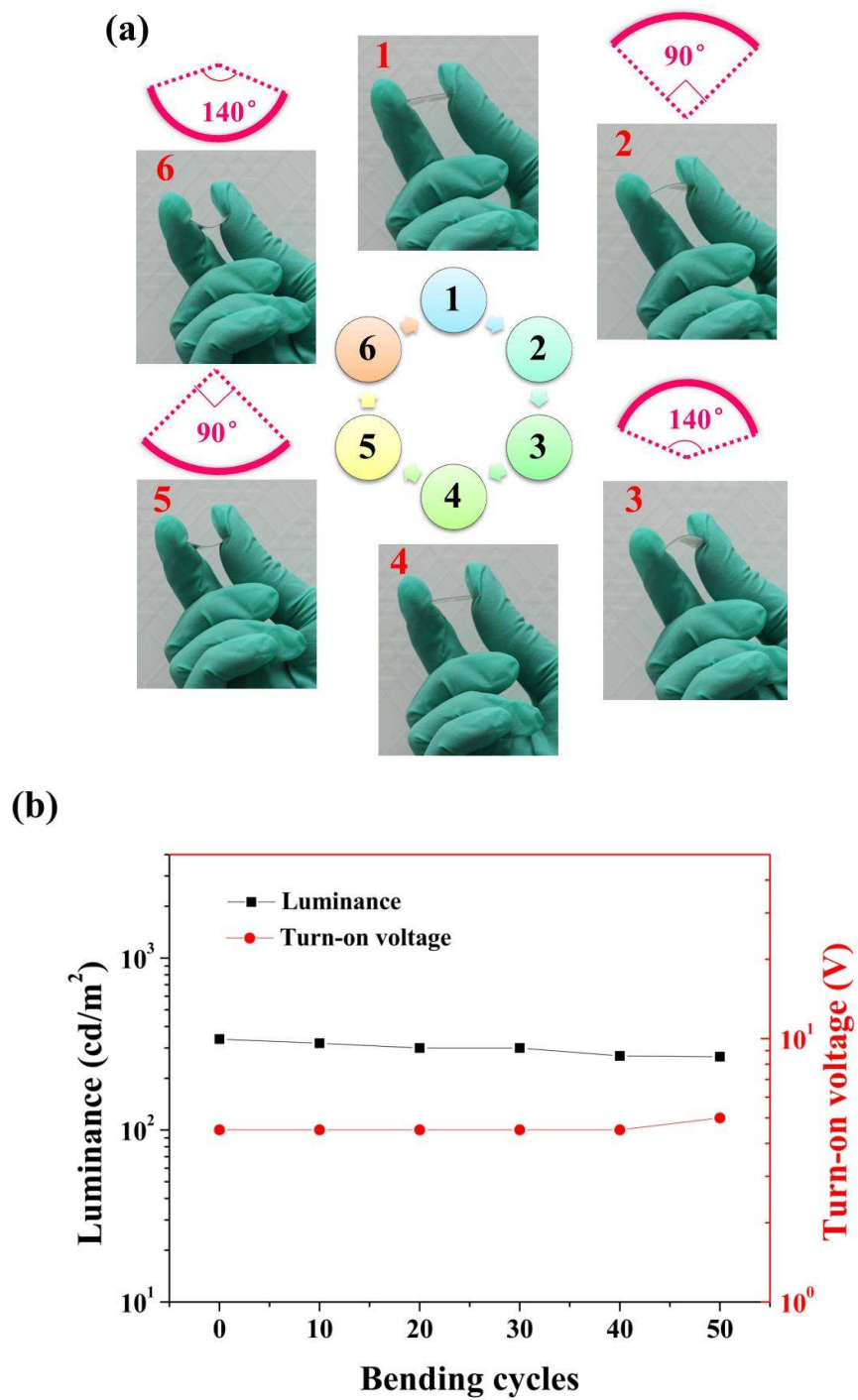


Figure 7

(S. Y. Jin et al., *submitted to J. Mater. Chem. C*)